

**WaPA**



Coastal and Open Ocean Surface Currents Mission Study:  
Wavemill Product Assessment  
ESA Contract: 4000107347/12/NL/AF  
Starlab Reference: WavemillPA-P20120327-01

Starlab Barcelona S.L.  
C. Teodor Roviralta 45,  
08022 Barcelona, Spain

## Wavemill Product Assessment

# Simulation of Wavemill Primary Scientific Products

Work Package	WP2200
Deliverable reference	D2.2
Date Completed	18/11/2014
Version	1.0

**Prepared by:** \_\_\_\_\_ **Date:** \_\_\_\_\_  
Starlab Wavemill Team

**Checked by:** \_\_\_\_\_ **Date:** \_\_\_\_\_  
José Márquez

**Approved by:** \_\_\_\_\_ **Date:** \_\_\_\_\_  
José Márquez

**Released by:** \_\_\_\_\_ **Date:** \_\_\_\_\_  
José Márquez

EUROPEAN SPACE AGENCY (ESA REPORT)  
CONTRACT REPORT

The work described in this report was done under ESA contract.  
Responsibility for the contents resides in the author or organisation that prepared it.

*The copyright in this document is vested in STARLAB Barcelona S.L. This document may only be reproduced in whole or in part, or stored in a retrieval system, or transmitted in any form (electronic, mechanical, photocopying or otherwise), only with the prior written permission of Starlab Barcelona SL.*

*Proprietary Information*

© Starlab Barcelona SL  
C/. Teodor Roviralta 45, 08022 Barcelona, Spain

*Commercial in Confidence*

[This page is intentionally left blank]

## AUTHOR/MANAGER/COLLABORATION LIST

Main Author(s)	Affiliation
Antonio Reppucci	Starlab Barcelona S.L.
José Márquez	Starlab Barcelona S.L.
Project Manager	Affiliation
José Márquez	Starlab Barcelona S.L.
Collaborator(s)	Affiliation
Bertrand Chapron	IFREMER

## DISTRIBUTION LIST

Distribution Record			
Sent to	Affiliation	Date	Format
Christopher Buck	ESA, ESTEC.	18 Nov. 2014	E-mail
David Cotton	SATOC	18 Nov. 2014	E-mail

## CHANGE RECORD

Change Record			
Issue	Date	Changes made	Author
0.1	12 March 2014	Preliminary draft version	A. Reppucci
1.0	18 Nov. 2014	Final Version	A. Reppucci

## Table of Contents

Index of Figures.....	5
Index of Tables.....	5
Acronyms and Abbreviations.....	6
Abstract.....	7
Keywords.....	7
1 Introduction.....	8
2 Validation Models.....	9
2.1 Q1: What is the spatial spacing you considered ? 1 m, 30 cm.....	9
2.2 Q2: Did you assign for each facet, the resulting local orbital velocity components, with local tilt angles ?.....	9
2.3 Q4: Did you evaluate the relative sensitivity of this solution to the local tilt changes?.....	10
2.4 Q5: Whatever the EM model, the fact that modulations are expected (at least from orientation changes) will contribute to change the cross section statistics from exponential (Rayleigh in amplitude) to heavier-tail distribution. Is that the case?.....	10
2.5 Q6: One aspect is certainly to take into account some modulations associated to hydro/aero effects. Even considering a 'toy' model, is it feasible to apply some modulation (on top of the tilt ones) to the cross section: correlation with the elevations and slopes of the dominant scales?.....	10
2.6 Q7: On the Doppler part: did you check that your mean Doppler (centroid or interferometric) is affected by the relative line-of-sight wind direction?.....	11
2.7 Q8: Do you implement interaction between current and ocean waves?.....	11
2.8 Q9: Do you check azimuth resolution loss (smearing) due orbital velocity?.....	11
3 Validation Tests.....	12
3.1 Doppler bias.....	12
3.2 Sensitivity of distribution's tail to wind and waves.....	13
3.3 Validation of Hydrodynamic modulation.....	13
3.4 Validation of azimuthal resolution loss.....	13
4 Validation Results.....	14
4.1 Clarification to Q1 ,Q2 and Q3.....	14
4.2 TEST-SIM-01.....	15
4.3 TEST-SIM-02.....	15
4.4 TEST-SIM-03.....	16
4.5 TEST-SIM-04.....	16
4.6 TEST-SIM-05.....	17
4.7 TEST-SIM-06.....	17
4.8 Clarification to Q6.....	18
4.9 Simulation of Wavemill Proof of concept campaign (PCC) data.....	18
4.10 Preliminary error budget.....	21
5 Conclusion.....	23
Bibliography.....	24

## Index of Figures

Figure 1 Scene definition.....	14
Figure 2 scene expansion to have power of two pixels.....	14
Figure 3 Doppler bias induced by increasing wind speed.....	15
Figure 4 Doppler bias induced by different wind directions.....	15
Figure 5 Doppler bias induced by different incidence angles.....	16
Figure 6 Doppler bias induced by swell with different wavelength.....	16
Figure 7 Histogram of NRCS for different wind speed (3 m/s dashed, 8 m/s dotted, 14 m/s continuous).....	17
Figure 8 (Left) contours of three point targets over the ocean surface for wind speed of 3 m/s (black) and 14 m/s (red). On the right side is shown the 3 dB contour line of the point target located at the center of the left image.....	17
Figure 9 (Left) Azimuthal correlation function for a wind speed of 14 m/s. (Right) plot of Azimuth cut off for different wind speed and fetch conditions.....	18
Figure 10: Magnitude of the hydrodynamic modulation function (red) along a wave profile (black).....	18
Figure 11: PCC spectrum.....	19
Figure 12: 2 D ocean current derived from PCC simulated data.....	20
Figure 13: 2-D currents derived from real data acquired during the PCC campaign.....	20
Figure 14 Doppler anomaly induced by different wind speed (red 3 m/s, green 7 m/s and black 14 m/s) as function of wind direction.....	21
Figure 15 Induced velocity bias induced by different wind speed (red 3 m/s, green 7 m/s and black 14 m/s) as function of wind direction.....	22

## Index of Tables

Table 3.1: Satellite configuration settings.....	12
Table 4.1 PCC simulation settings.....	19
Table 4.2 PCC simulation settings.....	21

## Acronyms and Abbreviations

2D	Two Dimensional
ADC	Analog-to-Digital Converter
ADCP	Acoustic Doppler Current Profiler
ATI	Along-track interferometry
DMSS	Directional MSS
DOC	Documentation
ECEF	Earth Centred - Earth Fixed
ESA	European Space Agency
FFT	Fast Fourier Transform
GEO	Geometry Module
GUI	Graphical User Interface
IDL	Interactive Data Language
INT	Interferometric Processing Module
INV	Inversion Module
IOR	Input/Output Requirements
LEO	Low Earth Orbit
LUT	Look Up Table
MSS	Mean-square Slope
NRCS	Normalized Radar Cross-section
OEF	Orbit Element File
PAM	Propagation and atmospheric Module
PCC	Proof-of-Concept Campaign
PRF	Pulse Repetition Frequency
RCMC	Range Cell Migration Correction
RF	Radio Frequency
RX	Receive
SAR	Synthetic Aperture Radar
SCT	Electromagnetic Scattering Module
SEA	Sea Generator Module
SIM	Simulator
SLC	Single-look Complex
SNR	Signal to Noise Ratio
SSH	Sea Surface Height Retrieval Module
SSM	Sea Surface Movement Retrieval Module
SWH	Significant Wave Height
TLE	Two-Line element file
TX	Transmit
WE2ES	Wavemill End-to-End Simulator
WGS 84	World Geodetic System - 1984
WIM	Wavemill Instrument Module
XTI	Cross-track interferometry

## **Abstract**

The objective of this document is to validate the outputs of the Wavemill End-to-End Simulator with respect to the models defined within the WP2100. This document contains the description of the tests to be performed for the validation of the Wavemill End-to-End Simulator in the framework of the algorithm assessment. For each test, a validation criteria is provided.

## **Keywords**

Wavemill, End-to-End Simulator, Interferometry, SAR, Ocean surface currents

## 1 Introduction

In the framework of the studies on the Wavemill concept, an End-to-End simulator has been developed in order to assess the different configurations and related sensitivity of a multi-beam wide-swath interferometric SAR instrument [1]. The simulator -developed by Starlab under ESA contract- is specifically designed to cope with this innovative concept-study and integrates all simulation, processing, and inversion steps involved in a real scenario. This includes the acquisition geometry, the sea state (including swell), the sea surface scattering, the atmospheric attenuation, and the instrument configuration (including monostatic and bistatic channels). In addition, the simulator provides a SAR/inSAR processing suit and a sea surface movement retrieval module.

Simulation of SAR images of the ocean surface is a complex task mainly because of the different geophysical phenomena (e.g. wave and current motion, wind, fetch, bathymetry, etc.) that affect the phase and amplitude of the produced data. In order to best represent all these effects on the simulated SAR data, the Wavemill End-to-end Simulator produces raw data by integrating the different phase and amplitude contributions of the scatterers, the geometry and instrument over the sea surface. This means that this simulator does not make use of analytical model transfer functions to generate the SAR images; keeping the generation process as simple and transparent as possible. However, the simulator does have to model the aforementioned geophysical phenomena (waves, currents, wind) and thus, these particular models should be properly defined and validated so that are well represented in the SAR images and the interferograms.

In the framework of this project, WP2100 has been devoted to the identification and modelling of the most representative geophysical phenomena affecting the SAR signal.

Main objective of WP2200 is to assess the scientific validity of the Wavemill primary products. This has been done through the following steps:

1. Theoretical analysis of the Wavemill measurement mechanism and determination of phenomena affecting the retrieved interferometric phase.
2. Modelling of the identified phenomena with respect to their impact on the interferometric phase.
3. Simulation of the identified phenomena from the proposed theoretical models.
4. Critical comparison of simulation results with data reported in past studies and campaigns.

In Section 2, there are compiled the different questions and validation models proposed by Bertrand Chapron in the context of WP2100. In Section 3, we present a summary of the planned validation tests; including a pass fail criteria. In Section 4, the results of the validation tests are presented. Finally, in Section 5, we present some conclusions and analysis of the validation results.



## 2 Validation Models

This section is a compilation of the discussion around the different validation models and tests proposed by Bertrand Chapron and extracted from the correspondence between Starlab and Ifremer on this topic. This correspondence has been the basis for the validation tests proposed in Section 3.

In this section:

- QX means Question X and makes reference to Bertrand Chapron original question.
- AX means Answer X and makes reference to Starlab answer to original question.
- CX means Comment X and makes reference to further comments of Bertrand with respect to the initial answer of Starlab.

### 2.1 Q1: What is the spatial spacing you considered ? 1 m, 30 cm

\_ The spatial spacing (pixel size) we consider in the simulation process is equal to the minimum between the azimuth and range posting, which are determined by the PRF and platform velocity in the first case and by the signal sampling frequency in the second case.

C1: So, given the PRF and/or the sampling frequency, what is the spatial spacing for the ocean scene ? Could you consider some wind dependency (to try to match resolved and unresolved facets with a standard 2 scale model).

As explained the ocean resolution is an input variable that can be set by the user as he thinks is better. There is only a limitation, the sampling can not be larger than the minimum between the azimuth and range posting

### 2.2 Q2: Did you assign for each facet, the resulting local orbital velocity components, with local tilt angles ?

A2: For each pixel the following parameters are considered in time (i.e. for each radar pulse generated):

- Pixel position over the ocean surface.
- Pixel velocity due to wave motion.
- Wind drift (equal to Bragg waves phase speed).
- Current velocity.
- Local incidence angle.

C2: In azimuth, the pixels are a posteriori results. So, one pulse is integrating a large band and the signal received at a given time is integrating over this band. Correspondingly, if you picture the band to be the collection of individual signals, the received signal will have a Doppler that already integrates the individual Doppler weighted by the scatter amplitude.

Accordingly, the Doppler at that time should already exhibit a change from the expected Doppler (geometry and platform speed). Is that so, and can you check this result ?

In particular, this is related to the mean correlation between the cross section changes due to local tilts, and individual line-of-sight velocity.

Is that ok ?

**Q3: What is then the solution you considered within the non-resolved patches?**

A3: For the computation of NRCS we used the composite model proposed in [1], (formulas 2 to 10). In detail we built a look-up table with NRCS values for a range of incidence angles (0°- 90°), and then we assign a value to each pixel depending on the local incidence angle.

C3: This is a 2-scale model. So did you decompose into 3-scale ? The one you resolved with local tilts, the one to further tilt the Bragg components, and finally the Bragg one.

The other around would be to consider the result of the 2-scale model applied to scales you did not resolved, and then to apply the local tilt transformation. This means to evaluate the slope variances of the resolved surface, then to remove them from the ones contributing to the 2-scale model.

Is this clear ?

**2.3 Q4: Did you evaluate the relative sensitivity of this solution to the local tilt changes?**

A4: We compare our results to the ones presented in [2] (see Figure 1). The difference close to nadir could be due to the different spectrum used (we used Elfouhaily [3]) or to the fact that we don't consider breaking waves contributions.

C4: Ok for the answer, but this is not really the question. For instance, could you check the results by artificially increasing the resolved tilts ? Say multiply or divide by 2, to check the consistency with your Doppler and Cross Section.

**2.4 Q5: Whatever the EM model, the fact that modulations are expected (at least from orientation changes) will contribute to change the cross section statistics from exponential (Rayleigh in amplitude) to heavier-tail distribution. Is that the case?**

A5: This was checked and it seems that the NRCS statistics do change in this way

C5: As the mean NRCS is changing between 3 to 8 and 14 m/s, I would expect the results you presented to go the other way around. But, I guess this is just a small mistake. Yet, this does not answer the question: I am asking the departure from Rayleigh distribution due to the modulation effects.

So, as related to previous question, can you check the sensitivity of the distribution tail to change in tilts at a given wind speed ? Then, can you check this sensitivity as the wind increases ?

When the wind is low, the NRCS is small (inside the unresolved facets) but shall be highly sensitive to local tilt changes. Thus, departure from Rayleigh must be quite pronounced. For high wind, the NRCS is large (inside the unresolved facets), and little affected by large scale tilts. So, contrary to low winds, departure from Rayleigh shall be less evident.

**2.5 Q6: One aspect is certainly to take into account some modulations associated to hydro/aero effects. Even considering a 'toy' model, is it feasible to apply some modulation (on top of the tilt ones) to the cross section: correlation with the elevations and slopes of the dominant scales?**

A6: As explained in the answer to Question 3, the simulator only takes into account contributions from Bragg and specular reflections (as at the time of the software design only these contributions were required). It is agreed that hydrodynamic modulation should be included, especially for wind speed retrieval. It would be useful to have a description of a "toy model" to implement this.

C6: You can simply suppose that the NRCS within the unresolved facets are  $x$  times larger over the crest of the longer dominant waves than at the troughs. So, you consider simply  $NRCS = NRCS_0 \cdot (1 + x \cdot h)$ , with  $x$  positive.

As such you can check again if the overall statistics are modified. As h is resolved, you can modify the phase of this modulation as you wish, and put more roughness in the front if you want. To obtain this effect, you simply rewrite:

$x^*h \rightarrow \int M(K) h(K) \exp(iK r) dK$ , with r the local position, and M(K) the Modulation Transfer Function in Fourier space. This MTF can be complex, and distributed over K. As such you can play to test different function and phase shifts.

More involved solution could be further considered by directly decompose NRCS into Fourier modes and then to apply a MTF. This would, for instance, take directly into account the tilt modulation.

## **2.6 Q7: On the Doppler part: did you check that your mean Doppler (centroid or interferometric) is affected by the relative line-of-sight wind direction?**

A7: Concerning the Doppler shift induced by near surface wind we did some tests using an ERS-2- like configuration (see Table 1) and looks that there is a Doppler anomaly induced by waves (tilt and motions), which depends on wind speed and direction. Please note that in the simulation process this anomaly is only induced by the longer waves; in addition we can add the Doppler due to the drift of Bragg scatterers, which is related to their phase velocity. This last contribution is directly added to the signal phase of each pixel.

C7: Did you check it, even when only considering no Doppler inside the unresolved facets ? Is this fully consistent with your inputs ?

## **2.7 Q8: Do you implement interaction between current and ocean waves?**

A8: The present implementation of the simulator does not take into account roughness distribution changes due to surface current variations, however we think it would be important in the future to include this effect.

C8: Ok. The simulation shall first consider the Doppler bias sensitivity to wind and wave effects.

## **2.8 Q9: Do you check azimuth resolution loss (smearing) due orbital velocity?**

A8: We will do tests in order to check the correct representation of this feature

### 3 Validation Tests

In order to execute the validation of the Wavemill simulator several test cases are envisaged. Each of these test cases is detailed in the following subsections. These tests have been defined in order to address the correspondence compiled in Section 2. In addition to these tests, we clarify Q1 and Q3 by providing a detailed description of the simulator implementation in Section 4.1.

For each test, plots of the more concerned parameters will be given depending on the characteristics of the feature that has to be studied.

The Platform/instrument setting used to run the tests is based on ERS 1/2 AMI sensors and orbit. The choice was dictated by the need of having literature references to compare the results. In Table 3.1, the settings used are presented.

Parameter	Value
PRF	1680.0 [Hz]
TX_BANDWIDTH	15549900.0 [Hz]
PULSE_DURATION	3.71200e-05 [ms]
CARRIER_FREQ	5.2966865e+09 [Hz]
SAMPLING_FREQUENCY	18963103.0 [Hz]
AZIMUTH ANGLE	0.0°
NOMINAL_ALTITUDE	777828.71 [m]
NOMINAL_VELOCITY	7480.9116

**Table 3.1: Satellite configuration settings**

#### 3.1 Doppler bias

This test will check that the Doppler bias due to ocean surface movements is correctly represented. The test aims to answer Q2, Q4 and Q7 detailed in Section 2.

TST-SIM-01	Simulation of ocean surface for different wind speed	The test will be executed for wind speed equal to [3,7,14,20] m/s and across track direction.
TST-SIM-02	Simulation of ocean surface for different wind directions	The test will be executed for wind directions equal to [90° (up wind), 135°, 180° (cross wind), 225°, 270° (down wind)]
TST-SIM-03	Simulation of SAR images at different incidence angles.	The test will be executed for a fixed wind speed (5 m/s) and direction (across track), and for incidence angle (at scene centre) of [20°, 30°, 40°].

TST-SIM-04	Simulation of ocean surface with different swell (tilts)	The test will be executed for a fixed wind speed (5 m/s) and direction (across track), and for for swell wavelength of [50,100,150,200] m.
------------	--	--

### Expected Results

Sea surface motion due to wind and waves induces a Doppler change from the expected one (the one obtained in case of static target). Plots of the Doppler bias for changes of wind waves and geometry will be shown.

### 3.2 Sensitivity of distribution's tail to wind and waves

The objective of the following tests is to check that the distribution's tail of SAR amplitude image changes as described in Q5 detailed in Section 2. This test will also answer to Q4 with regards to sensitivity of cross-section to local tilt changes.

TST-SIM-05	Simulation of ocean surface for different wind speed	For this test will be used the result of TST-SIM-02.
------------	--	--

TST-SIM-06	Simulation of ocean surface for different wind speed and swell	The test will be executed for wind speeds equal to [5, 20] m/s, across track direction, and with swell equal to [50, 200] m.
------------	--	--

### Expected Results

Image statistic departure from Rayleigh to havier-tail should decrease as wind speed increase. Plots of SAR image distribution will be shown.

### 3.3 Validation of Hydrodynamic modulation

This test will check that the implementation of hydrodynamic modulation model is correct. The test aims to answer the Q6 detailed in Section 2.

### Expected Results

Backscattering along long-waves profile has to change according to the proposed model. Plots of the backscattering values along a wave profile will be shown.

### 3.4 Validation of azimuthal resolution loss

This test will check that the azimuthal resolution loss (also called azimuth cut-off) is correctly represented by the simulator. The test aims to answer the Q6 detailed in Section 2.

TST-SIM-06	Simulation of ocean surface for different wind speed.	The test will be executed for wind speeds equal to [3,14] m/s and across track direction.
------------	---	---

## 4 Validation Results

This section includes the results of the tests proposed in Section 3. The results are evaluated against the pass / fail criteria defined also in that section.

### 4.1 Clarification to Q1 ,Q2 and Q3

To simulate SAR raw data the following stem are implemented:

1. First a scene is defined by its dimensions (along and across track) and sampling (pixel size) as shown in Figure 1

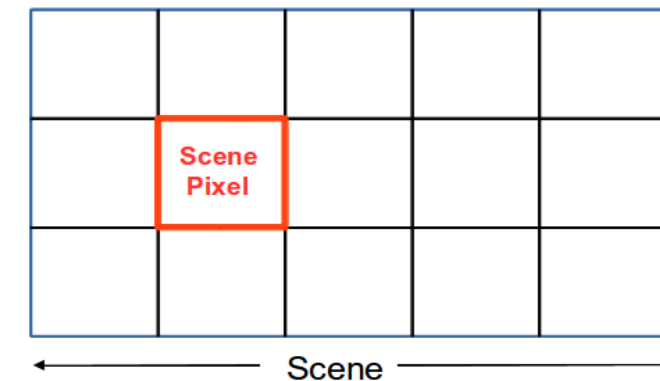


Figure 1 Scene definition

2. To speed up the processing the scene extension is expanded in order to have a number of pixel in range and azimuth equal to power of two (see Figure 2).

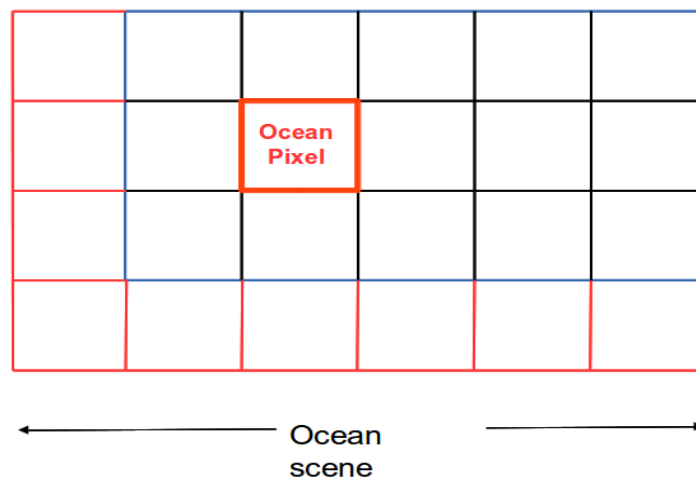
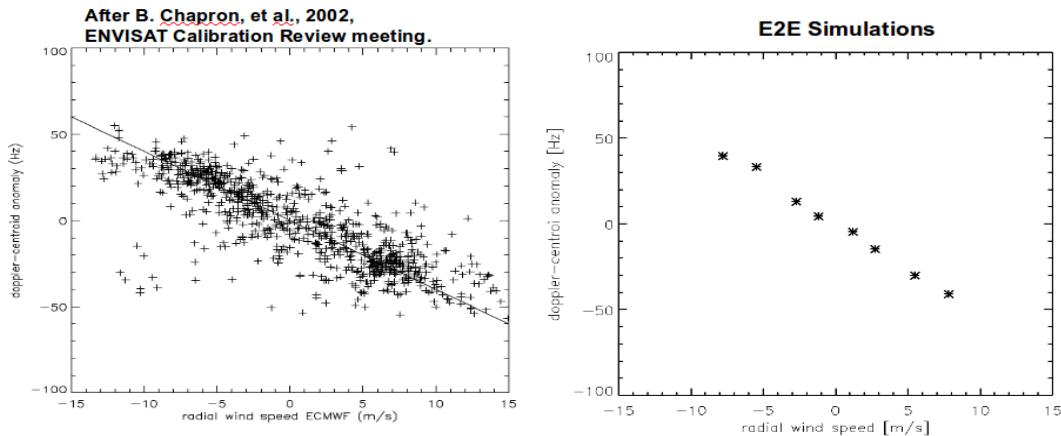


Figure 2scene expansion to have power of two pixels

3. For the computation of NRCS we used the composite model proposed in [2], (formulas 2 to 10). In detail we built a look-up table with NRCS values for a range of incidence angles (0°- 90°), and then we assign a value to each pixel depending on the local incidence angle.
4. A "Raw data" matrix is defined with dimensions and spacing dictated by the instrument configuration. Then for each pixel the following parameters are computed in time (i.e. for each radar pulse generated):

- Pixel position over the ocean surface.
  - Pixel velocity due to wave motion.
  - Wind drift ( equal to Bragg waves phase speed).
  - Current velocity.
  - Local incidence angle
5. As final step the antenna pattern is projected over the scene, and pixels that fall within it are integrated and stored in the “Raw data” matrix.

## 4.2 TEST-SIM-01



**Figure 3 Doppler bias induced by increasing wind speed**

Objective of the test is to check that the Doppler anomaly induced by different wind speed is correctly represented. In Figure 3 the E2E simulator results (on the right) are compared with real data (on the left). One can observe that the variation is the same. The test can be considered successful.

## 4.3 TEST-SIM-02

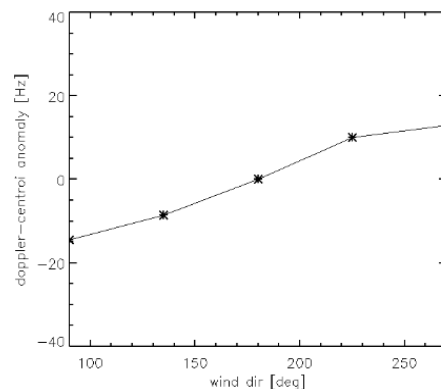


**Figure 4 Doppler bias induced by different wind directions.**

Objective of the test is to check that the Doppler anomaly induced by different wind directions is correctly represented. This is shown in Figure 4, where we can observe that, accordingly to the theory, the Doppler anomaly has absolute maxima for up/down wind directions (90°,270°) while is zero for crosswind (180°). The test can be considered successful.

#### 4.4 TEST-SIM-03

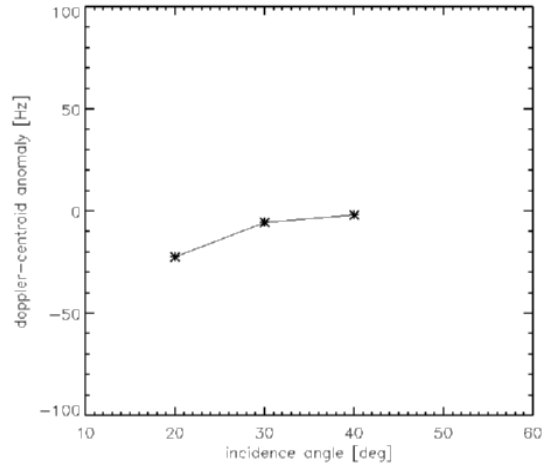


**Figure 5 Doppler bias induced by different incidence angles**

This test was planned to assess the correct behaviour of the induced Doppler anomaly with respect to changing incidence angles. Accordingly to [4] the Doppler anomaly increase with incidence angles (Figure 5). The test can be considered successful.

#### 4.5 TEST-SIM-04

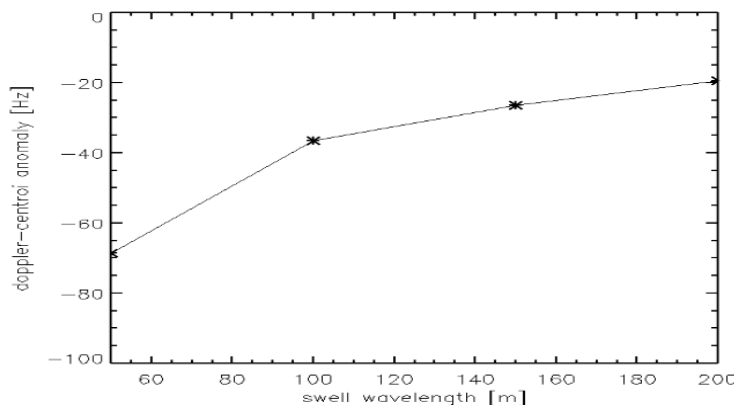


**Figure 6 Doppler bias induced by swell with different wavelength.**

According to theory [4] and increase of surface tilt lead to an increase of induced Doppler anomaly. To simulate this effect ocean surfaces with swell systems of different wavelength were simulated. In Figure 6 are shown the results.

The test can be considered successful.



#### 4.6 TEST-SIM-05

As explained in section 2.4 for low wind speed the backscattering is small, but very sensitive to local tilt changes, thus departure from Rayleigh must be quite pronounced. For high wind speeds this effect is less evident as the backscattering is large and little affected by large scale tilts. This is shown in Figure 7 where the histograms of the backscattering from ocean surface at different wind speeds are plotted. The test can be considered successful.

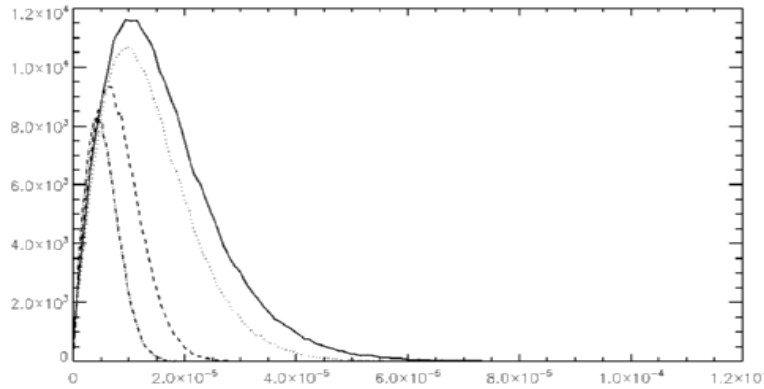


**Figure 7 Histogram of NRCS for different wind speed (3 m/s dashed, 8 m/s dotted, 14 m/s continuous)**

#### 4.7 TEST-SIM-06

Objective of this test was to check the azimuth resolution loss (smearing) due orbital velocity. In Figure 8 are shown the contours of point targets over the ocean surface for wind speed of 3 m/s (black) and 14 m/s (red); one can observe that at 14 m/s wind speed the point target is widened and shifted in along track direction. Additionally the SLC autocorrelation function (ACF) was computed to estimate the azimuthal cut-off wavelength. In Figure 9 on the right is shown the plot of the ACF for a wind speed of 14 m/s; the estimated value agrees with what reported in [5]. The test can be considered successful.

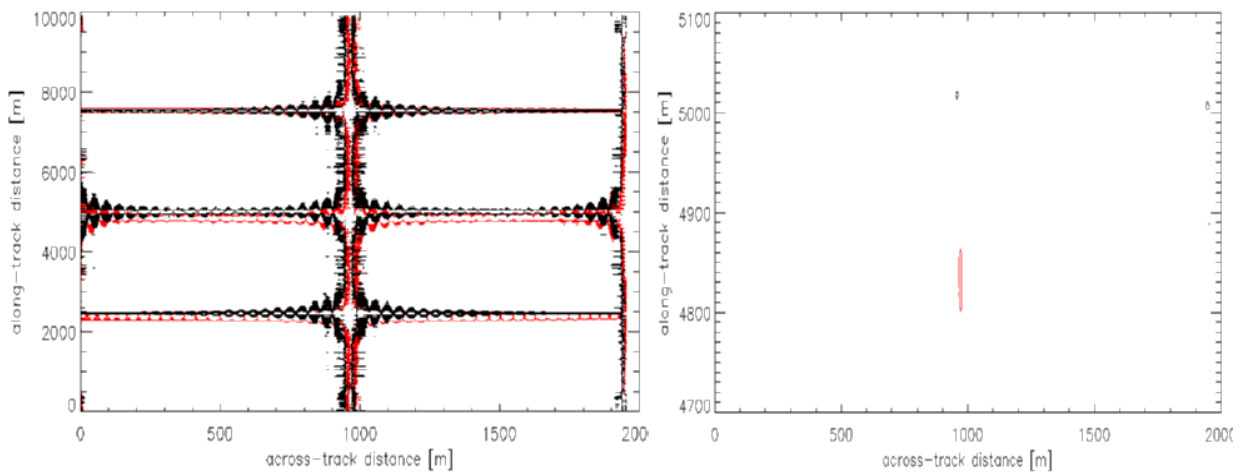


**Figure 8 (Left) contours of three point targets over the ocean surface for wind speed of 3 m/s (black) and 14 m/s (red). On the right side is shown the 3 dB contour line of the point target located at the center of the left image.**

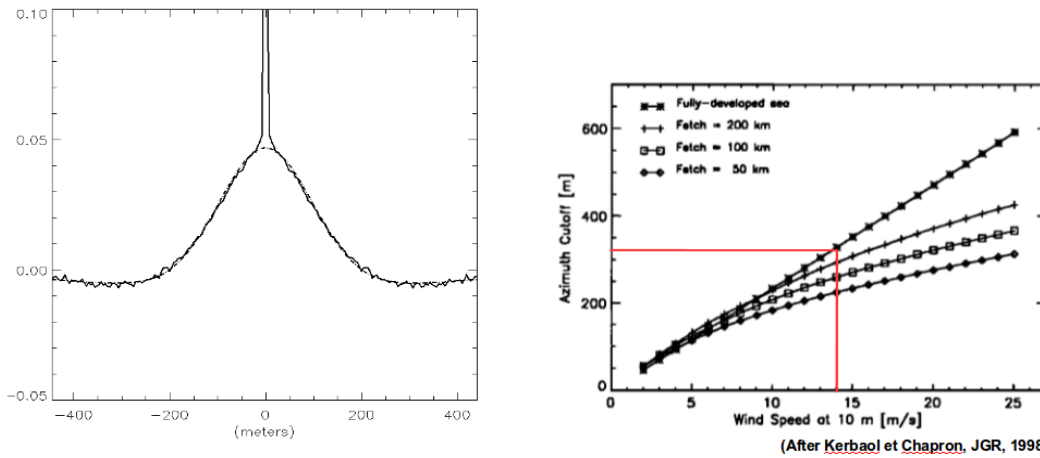


**Figure 9 (Left) Azimuthal correlation function for a wind speed of 14 m/s. (Right) plot of Azimuth cut off for different wind speed and fetch conditions.**

#### 4.8 Clarification to Q6

Hydrodynamic modulation was simulated as described in section 2.5. In Figure 10 in black is plotted a wave profile, while in red the magnitude of the hydrodynamic modulation function, which is maximum on the leading edge of the wave.

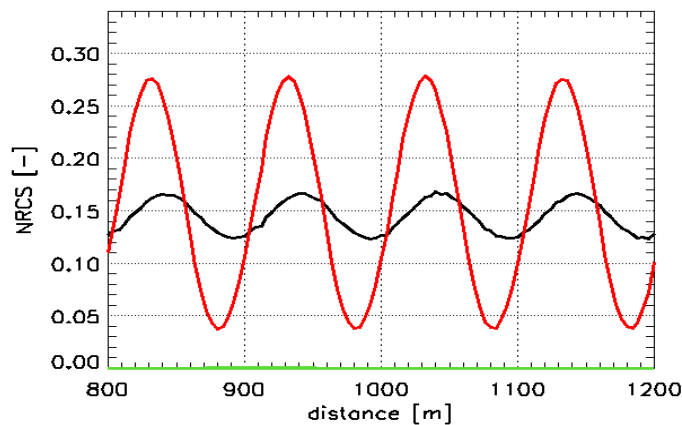


**Figure 10: Magnitude of the hydrodynamic modulation function (red) along a wave profile (black)**

#### 4.9 Simulation of Wavemill Proof of concept campaign (PCC) data

Once assessed the correct behaviour of the simulator, an additional test was done to simulate the data acquired during the campaign done in the framework of the PCC project.

To run the test an X band instrument and airborne platform has been simulated, like the one used for the PCC campaign. The setting parameters are detailed in Table 4.1.

Parameter	Value
PRF	700.0 [Hz]
TX_BANDWIDTH	1.3000000e+08 [Hz]
PULSE_DURATION	1.20000e-06 [ms]
CARRIER_FREQ	9.9999999e+09 [Hz]
SAMPLING_FREQUENCY	1.4950000e+08 [Hz]
AZIMUTH ANGLE	45.0°
NOMINAL_ALTITUDE	3000.0 [m]
NOMINAL_VELOCITY	250 [m/s]
INCIDENCE ANGLE	25°

**Table 4.1 PCC simulation settings**

The simulation of the ocean has been done using an ocean spectrum, provided by NOC, measured by a buoy located in the area covered by the PCC campaign; the short wave region has been filled using the analytic formulation proposed by Kudryatsev [xx]. In Figure 11, is shown a contour plot of the spectrum adapted to the coordinate system used by the simulator.

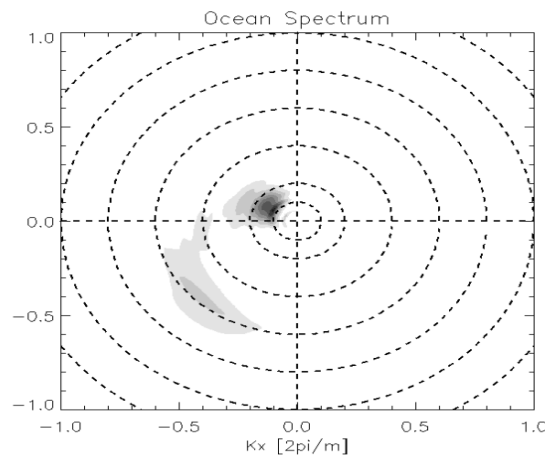


**Figure 11: PCC spectrum**

Wind and currents intensity and direction have been taken from a meteo-station and an ADCP instrument present in the area of interest.

In Figure 12 are shown the currents vectors for the simulated case, while in Figure 13 the ones estimated from the real data. The mean difference in direction between the two data is of 8° while the mean difference in magnitude is of 0.4 m/s.

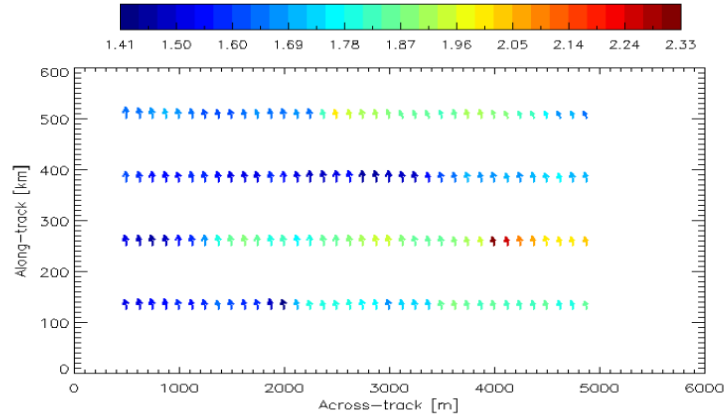


**Figure 12: 2 D ocean current derived from PCC simulated data**

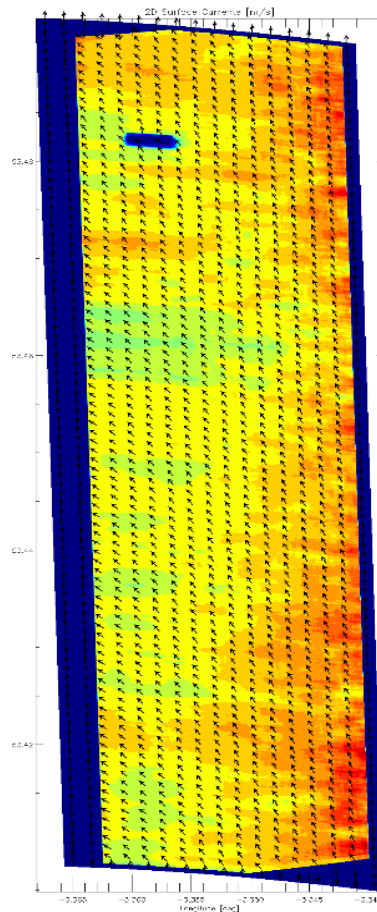


**Figure 13: 2-D currents derived from real data acquired during the PCC campaign**

### 4.10 Preliminary error budget

To quantify the effects of wave motions on the retrieval of the ocean surface currents vectors, a series of runs have been done for wind speeds equal to [3, 7, 14] m/s and directions equal to [0°, 45°, 90°]. Then the Doppler anomaly (i.e. the Doppler shift induced by wave motion) has been computed for each wind direction and speed.

The simulations were executed using a Ku band instrument and spaceborne platform. In Table 4.2 are detailed the setting parameters.

Parameter	Value
PRF	3200.0 [Hz]
TX_BANDWIDTH	60.000000e+06 [Hz]
PULSE_DURATION	7.40700e-05 [ms]
CARRIER_FREQ	1.1991698e+10 [Hz]
SAMPLING_FREQUENCY	66.00000e+06 [Hz]
AZIMUTH ANGLE	45.0°
NOMINAL_ALTITUDE	508226.13 [m]
NOMINAL_VELOCITY	7624.68 [m/s]
INCIDENCE ANGLE	20°

**Table 4.2 PCC simulation settings**

In Figure 14 is shown the plot of the induced Doppler anomaly for the different wind speeds (red 3 m/s, green 7 m/s and black 14 m/s) as function. The continuous lines are a fit using a sinusoidal function. In Figure 15 is plotted the velocity bias induced by waves movement.

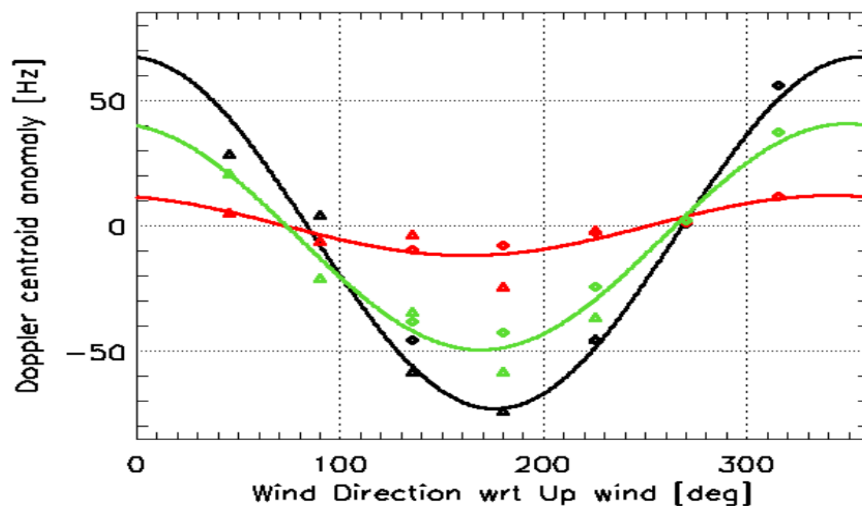


**Figure 14 Doppler anomaly induced by different wind speed (red 3 m/s, green 7 m/s and black 14 m/s) as function of wind direction**

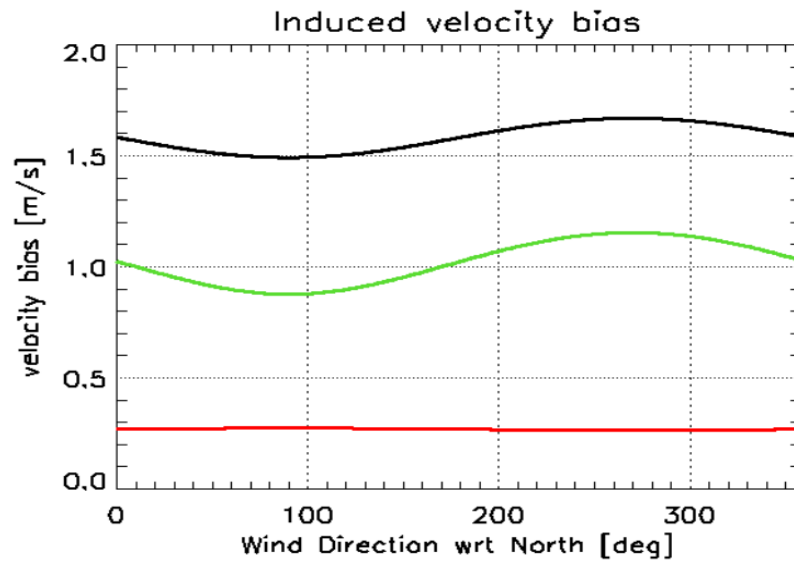


Figure 15 Induced velocity bias induced by different wind speed (red 3 m/s, green 7 m/s and black 14 m/s) as function of wind direction.

## 5 Conclusion

This deliverable describes the work done in the framework of WP2200, which aims at validating the outputs of the Wavemill End-to-End Simulator with respect to the models defined within the WP2100.

Several tests were planned following fruitful discussions with Ifremer.

The tests were focussed on:

1. The theoretical analysis of the Wavemill measurement mechanism and determination of phenomena affecting the retrieved interferometric phase.
2. The modelling of the identified phenomena with respect to their impact on the interferometric phase.
3. The simulation of the identified phenomena from the proposed theoretical models.
4. The critical comparison of simulation results with data reported in past studies and campaigns.
5. Preliminary error budget.

All the tests were executed successfully, proving that the simulator is able to reproduce all the sea-induced modulations of the backscattering, both in amplitude and phase.

In addition the code has been updated inserting a new routine for the simulation of the hydrodynamic modulation effect.

## Bibliography

- [1] Starlab Barcelona SL, *Executive Summary*, In Wavemill End-to-End Simulator, ESA ESTEC contract No. 4000103968, Version 1.0, 2 December 2013.
- [2] V. Kudryavtsev, D. Akimov, J. Johannessen, and B. Chapron, "On radar imaging of current features: 1. Model and comparison with observations", *Journal of Geophys. Res.*, 110, C07016, 2005.
- [3] Elfouhaily, T., Chapron, B., Katsaros, K., A unified directional spectrum for long and short wind-driven waves, *Journal of Geophysical Research*, Vol. 102, No. C7, July 1997.
- [4] A. A. Mouche, F. Collard, B. Chapron, K.-F. Dagestad, G. Guitton, J. A. Johannessen, V. Kerbaol, and M. W. Hansen, "On the use of doppler shift for sea surface wind retrieval from SAR," *Geoscience and Remote Sensing, IEEE Transactions on*, vol. 50, no. 7, pp. 2901–2909, July 2012.
- [5] Kerbaol V., Chapron B., Vachon P., "Analysis of ERS-1/2 Synthetic Aperture Radar Wave Mode images". *JGR* 1998.



[ END OF DOCUMENT ]